PHYSICAL REVIEW B VOLUME 45, NUMBER 16 15 APRIL 1992-II

Photoinduced-absorption investigation of oriented polymer systems: Polyacetylene and copolymer polyacetylene-polynorbornene

E. Mulazzi and A. Ripamonti
Dipartimento di Fisica dell'Università di Milano, via Celoria 16, 20133 Milano, Italy

T. Verdon and S. Lefrant
*Laboratoire de Physique Cristalline, Institut des Matériaux, Université de Nantes, 2 Rue de la Houssinière,
44072 Nantes CEDEX 03, France*

(Received 3 June 1991; revised manuscript received 17 December 1991)

We present polarized-photoinduced-ir-absorption data of oriented *trans*-$(\mathrm{CH})_x$ and triblock copolymers $(\mathrm{CH})_x$-(polynorbornene)$_n$-$(\mathrm{CH})_x$, for various x and n values. All spectra have been recorded by using polarized pump-and-probe beams, with polarizations perpendicular and parallel to the chain-stretching axis, respectively. The wavelengths of the pump beam are 514.5 or 351 nm. Among the different photoinduced features recorded in the polarized spectra, the broad ir band, whose maximum is reported at $\sim 500-600\ \mathrm{cm}^{-1}$, exhibits a more or less pronounced structured shape depending on the sample. To explain these features, we propose an interpretation in the framework of the perturbed Green-function method, leading to the determination of the localized photoinduced vibrational modes of the conjugated segments. The bimodal distribution of these segments, derived from the Raman data recorded from the same samples, is then used to weight the vibrational contributions to the photoinduced broadband from segments of different length.

In recent years, the electronic and vibrational properties of conducting polymers have been studied by using different techniques. In particular, the investigation of the photoinduced infrared absorption (PIA) performed on polyacetylene[1] has provided fundamental information on the photogenerated charges pinned at defect sites, through the photogenerated electronic low-energy (LE) absorption band peaked at $\sim 3500-4200\ \mathrm{cm}^{-1}$. Moreover, the photoinduced infrared vibrational modes observed at 500–600, 1282, and $1370\ \mathrm{cm}^{-1}$ are the signature of the perturbation induced by the photogenerated charges on the lattice dynamics of the conjugated segments. More recently, experimental data[2] obtained from Shirakawa $(\mathrm{CH})_x$ thin films have shown additional features in the PIA spectra. Very low intensity bands at 1034 and $1438\ \mathrm{cm}^{-1}$ can be observed. In addition another feature, peaked at $750\ \mathrm{cm}^{-1}$ in *cis*-rich $(\mathrm{CH})_x$, is recorded and is claimed to be derivativelike.[2] Notice that in the fully isomerized *trans*-$(\mathrm{CH})_x$, this feature appears as a more or less pronounced shoulder on the high-energy side of the main band peaked at $500-600\ \mathrm{cm}^{-1}$. This structure is supposed to be due to a thermal modulation of the absorption of remnant *cis*-$(\mathrm{CH})_x$ in the sample. The only ir absorption occurring in *cis*-$(\mathrm{CH})_x$ at this frequency is due to a (C-H) out-of-plane deformation mode whose frequency is at $740\ \mathrm{cm}^{-1}$ (see Ref. 3). Very recently, PIA spectra[4] have been carefully investigated on oriented $(\mathrm{CH})_x$ samples with different "*cis*" content: 50% and 100%, with the pump laser polarization perpendicular and the probe ir beam polarization parallel to the chain axis. In that work, the changes of intensities of the vibrational and electronic bands and their ratios, as function of the "*cis*" content and the pump laser frequency, are reported and discussed. Also, since the PIA spectra are polarized, an important observation concerning the peak at $750\ \mathrm{cm}^{-1}$ in the spectra of samples with different "*cis*" content is reported. As evidenced from the experimental data recorded with polarization parallel to the chain axis, this feature cannot be due to a thermal modulation of an absorption of *cis*-$(\mathrm{CH})_x$ due to the out-of-plane deformation mode at $740\ \mathrm{cm}^{-1}$. Nevertheless, no clear interpretation is proposed to explain the origin of this band.

In this paper, we report additional experimental data of polarized PIA spectra of oriented *trans*-$(\mathrm{CH})_x$ and oriented triblock copolymers polyacetylene-polynorbornene-polyacetylene, $(\mathrm{CH})_x$-$(\mathrm{NBE})_n$-$(\mathrm{CH})_x$ with different x and n values. Also, we report the theoretical interpretation of the vibrational features concerning the principal broad band (peaked at 500–600 cm^{-1}) in the PIA spectra of all these polymers, and for the *cis*-rich samples whose data have been published in Ref. 4. Our calculations are based on the model developed previously[5] for the photoinduced infrared bands. The model has been derived from the lattice dynamics of *trans*-polyacetylene, perturbed by the trapped photoinduced charges on different conjugated segments. In the present calculations, we have weighted the contribution to the photoinduced broadband coming from the perturbed vibrational frequencies of different conjugated segments by using the bimodal distribution derived from the analysis of the resonant-Raman-scattering (RRS) data[6–9] recorded from the same samples. Since in the calculations, the more important features are related to the main and broad photoinduced band (peaked at $500-600\ \mathrm{cm}^{-1}$ and extending up to $1050\ \mathrm{cm}^{-1}$) due to a large dispersion of the photoinduced vibrational frequencies in that frequency region, we are presenting here only the theoretical results concerning the shape of this band in different samples, while for the other vibrational bands we report only the values of the frequencies of the peak positions.

In Fig. 1, we present the experimental polarized PIA spectra recorded for different oriented polymer systems photoexcited with two laser wavelengths ($\lambda_{\text{pump}}=514.5$ and 351 nm). All the polarized spectra have been recorded with a FTIR Spectrometer (Nicolet 20 SXC) and in the following experimental conditions: the pump beam polarization is perpendicular and the probe beam polarization is parallel to the chain stretching axis. No signal has been recorded with the probe beam polarized perpendicularly to the stretching axis. The total power of the pump beam never exceeded 20 mW onto 20 mm^2 of the sample, maintained at 80 K, the laser light being chopped at 0.1 Hz. In our experiments, ten or twenty thousand scans were needed to obtain a reasonable signal-to-noise ratio. We compare in detail the experimental data mainly in the frequency range from 400 to 2000 cm^{-1}, the comparative analysis of the higher-energy part of spectra containing the LE band being only briefly discussed. In the frequency range considered here, the features for the different oriented samples are the following. In Fig. 1(a) (expt.), we present the PIA spectrum of fully *trans*-$(\mathrm{CH})_x$, pumped with $\lambda_{\text{pump}}=514.5$ nm. In this figure, the broad band is peaked at ~ 600 cm^{-1}, with a shoulder between 700 and 800 cm^{-1}. The other two well-known features are observed at 1287 and 1370 cm^{-1}, respectively, in agreement with previous data.[1,2] Note also that for this wavelength, the peak of the LE electronic band (not shown in the figure) is at ~ 0.51 eV. The PIA spectrum of the oriented copolymer $(\mathrm{CH})_x$-$(\mathrm{NBE})_n$-$(\mathrm{CH})_x$ (with $x=88$, $n=415$, and $\Delta l/l=5.3$) taken with $\lambda_{\text{pump}}=351$ nm, not shown in Fig. 1, presents electronic and vibrational features which are very similar to those reported above for *trans*-$(\mathrm{CH})_x$.

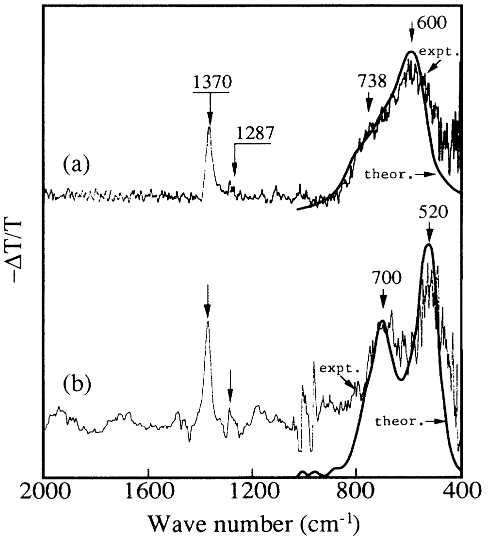

FIG. 1. (a) and (b) (expt.): experimental photoinduced ir spectra (400–2000 cm^{-1}) of oriented *trans*- $(\mathrm{CH})_x$ ($\lambda_{\text{pump}}=514.5$ nm) and $(\mathrm{CH})_{75}$-$(\mathrm{NBE})_{100}$-$(\mathrm{CH})_{75}$ ($\lambda_{\text{pump}}=351$ nm), respectively. Experimental spectra have been recorded at 77 K with the pump beam polarization perpendicular and the probe beam polarization parallel to the chain stretching axis. (a) and (b) (theor.): calculated band shapes in the frequency range 400–1000 cm^{-1}. The two sets of parameters are given in the text.

In Fig. 1(b) (expt.), the PIA spectrum of a stretched oriented copolymer $(\mathrm{CH})_x$-$(\mathrm{NBE})_n$-$(\mathrm{CH})_x$ (with $x=75$, $n=100$, and $\Delta l/l=3.5$) is given for $\lambda_{\text{pump}}=351$ nm. Notice that the peak of the broadband is significantly shifted to a lower frequency at ~ 520 cm^{-1}. Notice that in spite of interference effects observed in the spectrum, a second well-resolved component of the main band peaked at 700 cm^{-1} is observed with an intensity comparable to the one at 520 cm^{-1}. The other two sharp bands at 1287 and 1370 cm^{-1} are similar to those presented before. The peak of the LE electronic band is shifted to 0.58 eV with respect to that recorded in the PIA spectra of *trans*-$(\mathrm{CH})_x$.

The polarized RRS spectra of the previously discussed oriented polymers taken with different excitation wavelengths have been presented previously in Refs. 8 and 9. In particular, from the main features of those of $(\mathrm{CH})_{88}$-$(\mathrm{NBE})_{415}$-$(\mathrm{CH})_{88}$, we can derive, following the model of Refs. 6–9, the parameters of the bimodal distribution: $N_1=40$, $N_2=13$, $\sigma_1=20$, $\sigma_2=6$, and $G=0.45$. Let us recall that N_1 and N_2 refer to the number of double bonds for long ($N \geq 30$) and short ($N<30$) segments which are considered in the maxima of the double Gaussian distribution, respectively, whereas σ_1 and σ_2 are their standard deviations. G is the relative weight of the long-segment distribution. Then, from the analysis of the polarized RRS spectra of stretch-oriented *trans*-$(\mathrm{CH})_x$, we can deduce very close values for the above reported parameters since the polarized spectra are very similar to those discussed previously.

In order to explain the structured shape of the broadband peaked at 500–600 cm^{-1} and to calculate the photoinduced frequencies which contribute to the peak position of all the three vibrational bands observed in the polarized PIA spectra presented here, we follow the model developed in Ref. 5. In the framework of that model which uses the perturbed Green-function formalism, the perturbation, determined by the trapped charges at defect sites on the lattice dynamics of the conjugated segments, is taken into account through the parameter Λ. It represents the change of the force constants with respect to the unperturbed lattice dynamics of the conjugated segments in the polymeric chains. The vibrational frequencies induced by the perturbation are calculated by considering that the pinned charges at defect sites determine a positive change of the force constants of the lattice dynamics of the conjugated segments due to the change of the electron-vibration and electron-electron interactions. By following the perturbed Green-function method and the approximations performed applying this formalism to *trans*-polyacetylene, the density of perturbed vibrational states $\rho(\omega^2)$ is written in terms of Λ, $\bar{\rho}^0(\omega^2)$, and $\rho^0(\omega^2)$, which are the real and imaginary parts of the unperturbed Green function, respectively.[5]

As it is shown also in Ref. 10, where the study of the Raman-active doping-induced frequencies of n-type doped $(\mathrm{CH})_x$ is reported, there are different frequency regions where $\bar{\rho}^0(\omega^2)$ is considered and where the calculated perturbed mode frequencies are either more infrared or Raman active, according to the symmetry of the unperturbed modes which determine $\rho^0(\omega^2)$ and consequently $\bar{\rho}^0(\omega^2)$.

Following the procedure reported in Refs. 5 and 10, we find the localized vibrational mode frequencies which are photoinduced through the zeros of $1/\Lambda=\bar{\rho}^0(\omega^2)$, by considering the frequency regions where $\bar{\rho}^0(\omega^2)$ is positive and in which the new infrared active modes can be found. The evaluations of the shape of the broadband and of the other features in the PIA spectra of *trans*-$(\mathrm{CH})_x$ and triblock copolymers are performed by considering the plot of $\bar{\rho}^0(\omega^2)$ as a function of ω, which is calculated from long-segment lattice dynamics (Fig. 1, Ref. 5), and analogous diagrams for finite and short segments. The lowest average value of Λ we use here for the long segments is determined from the experimental value of the frequency of the principal peak ($\sim 500-600\ \mathrm{cm}^{-1}$) of the main band and of the peaks of the other two bands (~ 1287 and $\sim 1370\ \mathrm{cm}^{-1}$). The contributions to the broadband are determined by the various localized mode frequencies of the perturbed long- and finite-segment lattice dynamics, found by considering different values of Λ in the first frequency region of $\bar{\rho}^0(\omega^2)$ (see also Ref. 11). As it is shown in Fig. 1 of that reference, the photoinduced frequencies of the long and short segments are function of Λ and their behaviors are reported by the two different curves shown there.

The intensities of the different contributions of the photoinduced frequencies are calculated by considering the derivative of $\bar{\rho}^0(\omega^2)$, as reported in Ref. 5 and the ir transition dipole moments for the different conjugated segments of length N. These contributions to the band shape are then weighted by the bimodal distribution, which has been introduced to interpret and simulate the RRS and the optical-absorption spectra of *trans*-$(\mathrm{CH})_x$, in Ref. 6.

In Fig. 1(a) (theor.) we give the band-shape calculations ($400-1000\ \mathrm{cm}^{-1}$) performed by considering the Λ values starting from $2.10^6\ \mathrm{cm}^{-2}$ and the bimodal distribution determined by the analysis of the Raman data: $N_1=50$, $\sigma_1=10$, $N_2=14$, $\sigma_2=5$, and $G=0.5$. The peak of the PIA spectrum band at $\sim 600\ \mathrm{cm}^{-1}$ is due to the photoinduced frequencies of the perturbed long-segment lattice dynamics; the shoulder which can be noted at $740\ \mathrm{cm}^{-1}$ is due to the contribution of the short-segment photoinduced frequencies. This band shape is in very good agreement with the experimentally observed one reported in Fig. 1(a) (expt.) for stretched oriented *trans*-$(\mathrm{CH})_x$. Also, it reproduces well the band shape recorded in the PIA spectrum of the stretched oriented triblock copolymer characterized by $n=415$ and $x=88$ not shown in Fig. 1. This result is not unexpected since the polarized resonant Raman spectra of both stretched oriented polymers are very similar, as reported in Refs. 8 and 9, and consequently the bimodal distributions derived from that analysis are almost equal. By performing the calculations with the same parameter Λ, the other two vibrational bands turn out to be peaked at 1280 and $1370\ \mathrm{cm}^{-1}$.

In Fig. 1(b) (theor.) we show the calculated band shape with Λ starting from the value $1.8\times 10^6\ \mathrm{cm}^{-2}$ and the bimodal distribution characterized by $N_1=50$, $\sigma_1=10$, $N_2=13$, $\sigma_2=5$, and $G=0.35$. With these parameters, the principal peak of the band at $\sim 520\ \mathrm{cm}^{-1}$ and the secondary peak is well resolved with a maximum at $\sim 700\ \mathrm{cm}^{-1}$. This result is in excellent agreement with the experimental data reported in Fig. 1(b) (expt.) for the broadband in the polarized PIA spectrum of the stretched triblock copolymer $(\mathrm{CH})_{75}$-$(\mathrm{NBE})_{100}$-$(\mathrm{CH})_{75}$. In this calculation, the two other bands are peaked at 1278 and $1368\ \mathrm{cm}^{-1}$, respectively. Note that the secondary peak in the broadband is determined by the high weight of the short segments in the bimodal distribution.

We have performed the calculations with different parameters for Λ, starting from $2.1\times 10^6\ \mathrm{cm}^{-2}$ and for the bimodal distribution: $N_1=50$, $\sigma_1=10$, $N_2=10$, $\sigma_2=3$, and $G=0.3$. The evaluated band shape is shown in Fig. 2 and its maximum is found at $580\ \mathrm{cm}^{-1}$ with a well-resolved secondary peak at $750\ \mathrm{cm}^{-1}$. This band shape seems to reproduce well the one reported in Ref. 4 in the polarized PIA spectrum of oriented *cis*-rich sample at 50% concentration of "*cis*" isomers.

In this paper, we have presented the polarized PIA spectra of oriented polyacetylene and of triblock copolymers containing *trans*-$(\mathrm{CH})_x$ segments of different lengths and the theoretical interpretation of the band shape of the photoinduced ir broadband peaked at $500-600\ \mathrm{cm}^{-1}$ in different samples studied. By using the model proposed here, the shape of this band is interpreted by taking into account the photoinduced vibrational frequencies, calculated in the perturbed Green-function approximation, weighted by the conjugated segment dependent dipole moments parallel to the chain axis whose values are dependent on the length of the conjugated segments. In addition, the contributions to the band shape are also weighted by the bimodal distribution of the conjugated segments whose parameters are very close to those found from the analysis of the RRS spectra, recorded in polar-

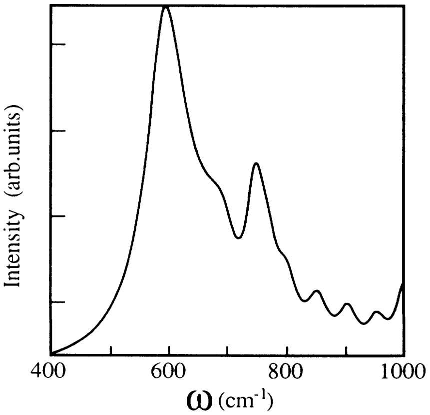

FIG. 2. Calculated shape for the vibrational photoinduced band in the frequency range $400-1000\ \mathrm{cm}^{-1}$; the parameters are given in the text.

ized light, of the same oriented sample.[8,9]

Following our interpretation, we propose that the observed structure at 740 cm^{-1} is due to the contribution of short-segment photoinduced frequencies and that the overall width of the bands comes from the distribution of conjugated segments present in the samples. It is well established[12] that *cis*-rich samples contain a high concentration of short segments in the "*trans*" part ($1-G=0.65-0.70$). For this reason, this structure is well pronounced in the photoinduced ir band (see Fig. 2). A similar result is obtained in the case of one of the triblock copolymers investigated [$(CH)_{75}$-$(NBE)_{100}$-$(CH)_{75}$], since the "*trans*" segments have a distribution similar to that present in the "*trans*" part of *cis*-rich samples [see Figs. 1(b) and 2]. On the contrary, in other investigated samples, the bimodal distribution shows a lower weight for the short segments ($1-G \sim 0.5$) and consequently the broadband in the PIA spectra exhibits only a more or less pronounced shoulder [see Fig. 1(a)]. This last feature of the photoinduced broadband disappears in the PIA spectra of very-high-quality *trans*-polyacetylene samples ($1-G \sim 0.3-0.25$), i.e., in the case of very low weight of the short-segment distribution. See also Ref. 13 for further discussions about this point.

Finally, we would also like to mention that the bimodal distribution of conjugated segments can qualitatively explain the change of the position of the maximum of the LE electronic band, which varies from 0.51 eV in fully *trans*-$(CH)_x$ to 0.58 eV in the copolymers characterized by a high percentage of short $(CH)_x$ segments. This effect was already reported in partially and fully isomerized Shirakawa samples,[2] where the change of the maximum of the LE band was pointed out. This is consistent with our analysis on the basis of the double distribution, for which a high weight of short segments induces an increase in the band-gap value and consequently a shift to higher energies of the LE band in the PIA spectra. This effect is then correlated to the secondary structure of the 500–600-cm^{-1} photoinduced band: the more pronounced the structure, the larger the shift to higher energies of the LE maximum with respect to the lowest value reported in the literature.[2]

One of us (E.M.) wants to thank the bilateral program CNR Italy/France for partial financial support. We wish also to thank Dr. G. Leising for stimulating discussions. The "Institut des Matériaux" is Unité Mixte de Recherches Centre National de la Recherche Scientifique/Université de Nantes No. 110.

---

[1] G. B. Blanchet, C. R. Fincher, T. C. Chung, and A. J. Heeger, Phys. Rev. Lett. **50**, 1938 (1983); Z. Vardeny, J. Orenstein, and G. L. Baker, *ibid*. **50**, 2032 (1983).

[2] H. E. Schaffer, R. H. Friend, and A. J. Heeger, Phys. Rev. B **36**, 7537 (1987).

[3] H. Shirakawa and S. Ikeda, Polym. J. **2**, 231 (1971).

[4] K. Pichler and G. Leising, Europhys. Lett. **12**, 533 (1990).

[5] G. P. Brivio and E. Mulazzi, Solid State Commun. **60**, 203 (1986).

[6] G. P. Brivio and E. Mulazzi, Phys. Rev. B **30**, 676 (1984).

[7] E. Faulques, E. Rzepka, S. Lefrant, E. Mulazzi, G. P. Brivio, and G. Leising, Phys. Rev. B **33**, 8622 (1986).

[8] E. Mulazzi, G. Leising, F. Stelzer, T. Verdon, and S. Lefrant, Synth. Met. **41**, 1333 (1991).

[9] S. Lefrant, T. Verdon, G. Leising, and E. Mulazzi, in *Frontiers of Polymer Research*, edited by P. N. Prasad and J. K. Nigam (Plenum, New York, in press).

[10] E. Mulazzi, S. Lefrant, E. Faulques, and E. Perrin, Synth. Met. **24**, 35 (1988).

[11] G. P. Brivio and E. Mulazzi, Synth. Met. **17**, 273 (1987).

[12] E. Perrin, E. Faulques, S. Lefrant, E. Mulazzi, and G. Leising, Phys. Rev. B **38**, 10 645 (1988).

[13] E. Mulazzi, A. Ripamonti, and S. Lefrant, Synth. Met. **41**, 1337 (1991).